Cross-flow microfiltration of wine: Effect of colloids on critical fouling conditions

Youssef El Rayess, Claire Albasi, Patrice Bacchin, Patricia Taillandier, Martine Mietton-Peuchot, Audrey Devatine

HAL Id: hal-00750746
https://hal.science/hal-00750746

Submitted on 12 Nov 2012

Cross-flow microfiltration of wine: Effect of colloids on critical fouling conditions

Y. El Rayess [a,b,*], C. Albasi [a,b], P. Bacchin [c,d], P. Taillandier [a,b], M. Mietton-Peuchot [e,f], A. Devatine [e,f]

[a] Université de Toulouse; INPT, UPS; Laboratoire de Génie Chimique; 4 Allée Emile Monso, F-31432 Toulouse, France
[b] CNRS; Laboratoire de Génie Chimique; F-31432 Toulouse, France
[c] Université de Toulouse; INPT, UPS; Laboratoire de Génie Chimique; 118 Route de Narbonne, F-31062 Toulouse, France
[d] CNRS; Laboratoire de Génie Chimique; F-31062 Toulouse, cedex 09, France
[e] Université de Bordeaux, ISVV, EA 4577, Unité de recherche OENOLOGIE, 33882 Villenave d'Ornon, France
[f] INRA, ISVV, USC 1219 OENOLOGIE, 33882 Villenave d'Ornon, France

* Corresponding author at: Université de Toulouse; INPT, UPS; Laboratoire de Génie Chimique; 4 Allée Emile Monso, F-31432 Toulouse, France.
Tel.: +33 534323626.
E-mail address: youssef.elrayess@ensiacet.fr (Y.E. Rayess).

ABSTRACT

Critical fouling conditions were studied during wine cross-flow microfiltration using a multichannel ceramic membrane (0.2 μm). The aim was to determine critical operating conditions in order to limit fouling caused by wine colloids (tannins, pectin and mannoproteins) and enhance process performances. The method used is a square wave filtration based on the determination of the reversibility and irreversibility of fouling. Filtrations were performed with filtered red wine (FW) added with different concentrations of colloids. Considering FW, critical flux for irreversibility was beyond the studied range of pressure ($\geq 1.4 \times 10^{-4}$ m/s). No clear critical flux could be determined for any of the tested molecules in the studied range of pressure. On the other hand, an upper limit of fluxes range has been identified (below which critical flux could be found). Irreversible fouling always takes place from the beginning of the filtrations and even at low pressures. For FW containing 0.2 g/l mannoprotein and 0.5 g/l pectin, a loss of average fluxes is observed beyond a given limit of transmembrane pressure. This fact was attributed to the compaction of a gel layer. Finally, a criterion ($R_{if}/R_m \leq 1$) has been suggested to determine the so-called "threshold flux" below it, fouling remains acceptable.

Keywords:
Cross-flow microfiltration
Wine colloids
Critical flux
Polysaccharides
Tannins

1. Introduction

After alcoholic and malolactic fermentations, the crude wine is a complex medium presenting a turbid aspect that is not well accepted by the consumer; therefore, it needs to be clarified. In order to have a limpid wine, the wine makers implement successive solid–liquid separations using traditional technologies such as centrifugation, dead-end filtration (filter presses, filtration on sheets, diatomaceous earth filtration) and the use of exogenic additives.

Nowadays, diatomaceous earth is classified as dangerous substances due to the presence of crystalline silica [1]. Diatomaceous earth has also a negative impact on environment; after uses, it cannot be disposed but it must be transported to waste disposal sites to be treated. So, environmental and health restrictions force the oenology sector to search for alternative techniques to traditional filtrations. Cross-flow microfiltration could then represent this alternative. Indeed, this technology can substitute a one-step procedure to the conventional processes which imply several filtration steps on diatomaceous earth previous to the final microbial stabilization obtained by dead end filtration on sheets or membranes [2]. In addition to a great simplification of the wine processing line, cross-flow microfiltration offers a number of additional advantages such as elimination of earth use and its associated environmental problems as well as the combination of clarification, stabilization and sterile filtration in one single continuous operation.

Conventionally, the cross-flow microfiltration development in wine filtration has long been hampered by significant fouling of the membrane. Poor performances, high costs, and risk of excessive retention of some components are the main consequences of fouling, leading sometimes to a loss of some organoleptic characters. Membrane fouling during filtration of complex fluids such as fermented food products (wine, beer) is the result of interplay of several mechanisms. These latter could be divided into [3,4]:

Internal fouling by small particles and colloids as adsorption and pore plugging within the internal structure of pores;
External fouling by particles, macromolecules and macromolecules aggregates as pore blocking and cake formation

The main drawback in wine filtration lies in the difficulty to understand wine filterability and the reproducibility of the filtrations. Many advances have been made by researchers especially

in identification of wine components responsible of fouling and in impact of membrane materials [5–10]. But, there still a lack of knowledge of the mechanisms causing fouling. The influence of the operating conditions on these mechanisms is then non-elucidated and mastering the process is not easy.

Membrane surface fouling could be characterized with regard to its reversibility. A reversible accumulation will be removed when the transmembrane pressure is decreased. An irreversible deposition will be removed only by a physical or chemical cleaning and will remain when the pressure is released. The limit between reversible and irreversible fouling depends on the flux value. The threshold value for which the reversible fouling turns into irreversible fouling is called as "critical flux" [11].

In food industry, there were many attempts to determine a critical flux. Gésan-Guiziou et al. [12] showed while cross-flow microfiltration of skimmed milk that a critical ratio of permeate flux over wall shear stress could be determined $(0.9 \, \text{l/h/m}^2/\text{bar})$ above it an irreversible deposition is observed. Youravong et al. [13] evaluated the critical flux in ultrafiltration of skimmed milk by plotting critical flux versus the ratio of wall shear stress over protein concentration. They showed a linear relationship between critical and wall shear stress/protein concentration. De Brujin and Borquez [14] showed that no critical flux was reached during ultrafiltration of apple juice with their operating conditions. But, their simulations have showed that no cake formation was observed at a tangential velocity of 7.4 m/s and transmembrane pressure of 150 kPa $(J_{\text{critical}} = 6.8 \times 10^{-5} \, \text{m/s})$. The filtration conditions used in these works (very high temperature 50–55 °C, very high tangential velocity up to 7 m/s) cannot be applied to wine filtration because it would have hugely modified wine quality.

The objective of this study is to investigate and search for some critical operating conditions in wine cross-flow microfiltration. It has been identified that substances like polysaccharides (pectin and mannoproteins), polyphenols and proteins are involved in membrane fouling [5–9] but little information concerning the individual impact on fouling and the mechanisms involved are available. The aim of this study is to limit fouling due to wine colloids (tannins, pectin and mannoproteins) and enhance process performances. The chosen study protocol was to evaluate the critical fouling conditions for each of the fouling molecules. This situation does not represent a real wine but it is a first step towards understanding real wine critical filtration conditions. The method used was a square wave filtration which allows the determination of the extent of fouling reversibility during wine cross-flow microfiltration. This method enabled the distinction between reversible and irreversible fouling as well as the calculation of a more accurate value of the critical flux.

2. Background

The first definitions of the critical flux concept appeared in 1995. The critical flux concept was defined as "the flux below which no fouling occurs" [15], as "the flux below which a decline of flux with time does not occur; above it fouling is observed" [16] or as "a flux below which there is no fouling by colloidal particles" [17].

There are two forms of critical flux: strong and weak forms [16,18]. The strong form is the flux at which the transmembrane pressure starts to deviate from the pure water line, which is of course linear. The strong form of critical flux has been developed to discriminate no fouling conditions. The weak form of critical flux is characterized by a very rapid fouling on the start-up and the flux-transmembrane pressure relationship is below that of the pure water line. The weak form of critical flux is the point at which this line becomes non-linear.

In 2006, Bacchin et al. [11] refined the definitions of critical flux and another term has been added as critical flux for irreversibility J_{ci}. This term was explained by the transition between concentration polarization layers to the deposit layer. Fig. 1, as seen by authors, illustrates the concept of this critical flux for irreversibility. When filtering at a flux below the critical flux, the colloidal system is usually stable as the result of repulsive interactions (interparticle or particle-membrane) overcoming the drag force (induced by the movement of solvent through the membrane). Beyond a given value of permeate flux (critical flux), when the repulsive forces are overwhelmed by the drag forces, a deposit appears and creates hydraulic resistance. This phenomenon of deposit formation is not instantaneous and may take several minutes to several hours to settle depending on the operating conditions and the type of particles.

Mathematically, the irreversibility form of critical flux (J_{ci}) can be defined by:

$$\text{For } J < J_{\text{ci}} : J = \frac{\Delta P - \Delta \Pi}{\mu(R_{\text{m}})} = \frac{\Delta P}{\mu(R_{\text{m}} + R_{\text{rf}})} \text{ or } \frac{\Delta P}{\mu(R_{\text{m}} + R_{\text{ads}} + R_{\text{rf}})},$$

if adsorption takes place (1)

where J is the permeate flux, ΔP the transmembrane pressure (Pa), $\Delta \Pi$ the osmotic pressure (Pa), μ the permeate viscosity (Pa s), R_{m} the membrane hydraulic resistance (m^{-1}), R_{ads} resistance due to adsorption (m^{-1}) and R_{rf} the reversible resistance (m^{-1}).
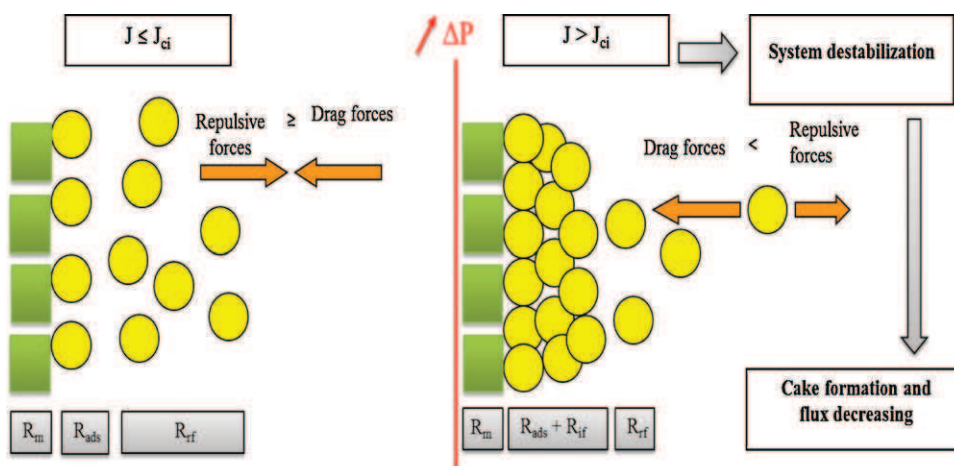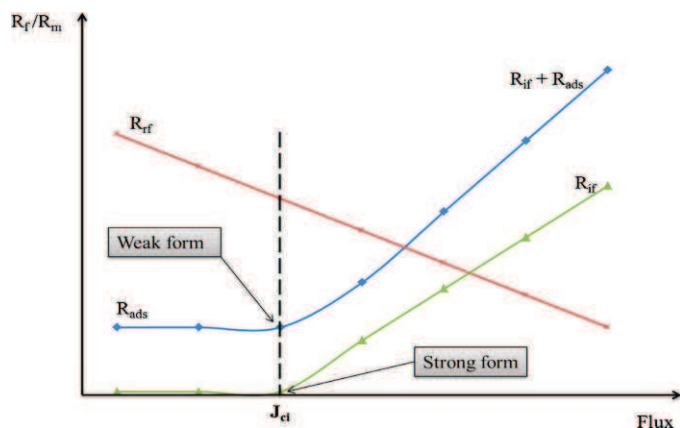

Fig. 1. Diagram representing the state of colloidal system at different flux values where R_{m} = membrane resistance, R_{ads} = resistance due to adsorption, R_{rf} = reversible resistance and R_{if} = irreversible resistance.

Fig. 2. Schematic representation, as seen by authors, of the critical flux of irreversibility and its relationship with the strong form and weak form of critical flux (R_f = fouling resistance).

The reversible accumulation of matter, after a decrease in pressure, is related to the polarization layer and its induced osmotic pressure. This latter act as an opposite force to the applied pressure. In this case, the reversible resistance associated with the polarization concentration layer can be treated as a term of osmotic pressure.

Above the critical flux for irreversibility, multi-layers of irreversible fouling are detected in the boundary layer whereas below it only a concentration of polarization layer exists in all cases with an additional monolayer of adsorbed species in some cases [11,19].

$$\text{For } J > J_{\text{ci}} : J = \frac{\Delta P - \Delta \Pi}{\mu(R_{\text{m}} + R_{\text{if}})}$$

$$= \frac{\Delta P}{\mu(R_{\text{m}} + R_{\text{rf}} + R_{\text{if}})} \text{ or } \frac{\Delta P}{\mu(R_{\text{m}} + R_{\text{ads}} + R_{\text{rf}} + R_{\text{if}})},$$

if adsorption takes place (2)

where R_{if} is the irreversible resistance (m^{-1}).

Fig. 2, as seen by authors, illustrates the relationship of the different forms of critical flux and the resistance presented in Eqs. (1) and (2). The strong form is the "ideal" case where the irreversible resistance below the critical flux is equal to zero. Beyond the value of the critical flux for irreversibility, the irreversible resistance becomes detectable. In other hand, the weak form is characterized by a given value of resistance for low fluxes due to the adsorption of molecules on membrane material. The critical flux for irreversibility is determined when the irreversible resistance becomes higher than that of the adsorption. Simultaneously to these variations, there is generally a decrease in the reversible part of fouling (R_{rf}) when the flux increases.

Recently, a new notion has appeared known as "sustainable flux" which includes economical factors [11,20]. This notion was found because for some systems operating at a zero fouling condition is simply not feasible. This concept was especially used for the treatment of complex fluids as wastewater treated by membranes bioreactors [20–22].

3. Materials and methods

3.1. Red wine

The red wine used in the present study was elaborated in 2008 at the cooperative cellar of Rabastens (France) from Duras, Fer Servadou and Syrah grape varieties. Thermovinification process was used to elaborate this wine in order to increase the extraction of polyphenolic compounds. After alcoholic and malolactic fermentations, the wine was centrifuged at the cellar in order to remove microorganisms and particles. A filtration was performed with a cross-flow microfiltration pilot plant equipped with organic membrane having an average pore size of 0.2 μm. The wine is analyzed and maintained at 4 °C until use to prevent microorganisms' development. Prior to experiments, a second filtration is performed with the filter used for this study (cf. Section 3.4) in order to eliminate eventual potassium tartrate crystals and precipitates. This final step allows obtaining the filtered wine (FW). The filtered wine used for all filtrations has 12% as alcohol content, 3.6 as pH, 0.6 g/l as sugars (glucose + fructose) and 0.1 g/l as malic acid.

3.2. Chemicals

Tannins (Biotan®) were purchased from Laffort (Bordeaux, France). These tannins are proanthocyanidic tannins extracted from grape skin with instantaneous dissolving. They were added to the wine (FW) with the concentrations of 1.25 g/l and 2.5 g/l. Pectin was purchased from Sigma–Aldrich (Lyon, France) and used at a concentration of 0.25 g/l and 0.5 g/l. Mannoproteins (Mannostab®) were purchased from Laffort and added to the wine at concentrations of 0.1 g/l and 0.2 g/l. The concentrations of added molecules are chosen according to those found in wine and identified in the literature [24,25].

3.3. Wine components analysis

Spectrophotometric analyses were carried out on an Agilent 8453 UV/VIS spectrophotometer. Total polyphenols in wine were estimated by the Total Polyphenol Index (TPI) using the absorbance at 280 nm and under 1 cm optical path. Colour Intensity (IC) is the sum of optical densities at 420 nm, 520 nm and 620 nm under 1 mm optical path. Total polysaccharides were determined using the modified Usseglio-Tomasset method based on the precipitation of the polysaccharides with ethanol [23]. Mannoproteins were also determined using the modified Usseglio-Tomasset method. Total anthocyanins were determined according to Ribéreau-Gayon method using the sodium bisulphite [24]. Total tannins were also determined according to Ribéreau-Gayon method by transforming the proanthocyanidins into anthocyanidins [24]. pH, % of alcohol, malic acid, glucose and fructose concentration were determined on the wine by FTIR spectroscopy (Fourier transform infra-red spectroscopy). Wine viscosity is determined with a controlled-stress rheometer (AR-2000 ex). Turbidity measurements (NTU) were performed with a Eutech TN-100 turbidimeter.

Table 1 shows the analytical composition of the wine before adding molecules (FW) and after adding molecules. A net increase in TPI, IC and turbidity is observed after addition of tannins. It should be noted that about 80% of total tannins are found after adding tannins powder. This was explained by the assays conducted on tannins powder which show that it contains 80% tannins and is free of polysaccharides. The other compounds are organic acids, sugars, minerals and vitamins which are not involved in membrane fouling during microfiltration. On the other side, the determination of total polysaccharides in wines FW + pectin and FW + mannoprotein shows that the amounts of measured polysaccharides are equivalent to those added [24,25].

3.4. Experimental apparatus

The filtrations were performed with a wine filtration pilot system (Fig. 3) designed for this study and provided by Pera Company (Florensac, France). The equipment consists of a 10 l stainless steel feed tank, a centrifugal pump (for a better respect of wine quality), an electronic flow-meter to measure the axial feed flow rate, 2 temperature sensors (T_1 and T_2) and 3 pressure sensors located at the

Table 1
Analytical composition of wine added with tested molecules.

	TPI	Total anthocyanins (mg/l)	Total tannins (g/l)	Total polysaccharides (mg/l)	IC	Turbidity (NTU)
FW	44.9 (±0.5)	349 (± 3.42)	2.45 (± 0.16)	60(± 30)	0.88 (± 0.07)	0.1 (± 0.2)
FW + 1.25 g/l tannins	59	355	3.49 (±0.1)	64	0.93	38.7
FW + 2.5 g/l tannins	73	360	4.45 (±0.15)	68	0.99	72.5
FW + 0.25 g/l pectin	45.1	n.d.	2.45	320	0.85	12.2
FW + 0.5 g/l pectin	44.7	n.d.	2.4	510	0.85	18
FW + 0.1 g/l mannoprotein	44.8	n.d.	2.46	165	n.d.	4.5
FW + 0.2 g/l mannoprotein	44.5	n.d.	2.45	275	0.84	8.5

feed tank entrance (P_1), at the inlet (P_2) and at the outlet (P_3) of the membrane module. Transmembrane pressure (ΔP) was calculated as $\Delta P = (P_2 + P_3)/2$. The pressure in the system is obtained with compressed air that pressurizes the feed tank. The pressure is accurately regulated in the pilot by a current to pressure transducer controlled with a computer software interface. A digital balance, connected to the system, was used to determine the evolution of permeate mass within the time and to calculate the permeate flux. A data acquisition system was connected to the microfiltration pilot: it allows the continuous monitoring of ΔP, temperatures and permeate mass along the time.

The microfiltration module contains a multi-channel (44) ceramic membrane (BK-Kompact, Novasep, France) shown in Fig. 3. Its average pore diameter is 0.2 μm. The total active membrane surface was 0.118 m², with an external diameter of 25 mm. The membrane is made of ZrO_2/TiO_2 layers laid on monolithic TiO_2–Al_2O_3 support layer. The flow velocity is fixed at 2 m s⁻¹ which is conventionally used in wine filtration.

After each experiment, a 6 steps procedure of chemical cleaning is performed to regenerate the membrane. This procedure is summarized in Table 2. The membrane permeability is checked with osmotic water after chemical cleaning and must be equal

Table 2
Chemical cleaning procedure after filtration experiment.

Step	Action
1	Rinsing membrane with water (5 min)
2	Rinsing membrane with warm water (45–50 °C) + 0.5% NaOH (10 min)
3	Rinsing membrane with hot water (75–80 °C) + 2–4% NaOH (15 min)/Filtration
4	Rinsing membrane with warm water (45–50 °C) (10 min)/filtration
5	Rinsing membrane with water (20–25 °C) + 0.2% citric acid (10 min)/filtration
6	Rinsing membrane with water (20 °C) (5 min)/filtration

or above 900 l/h/m²/bar (at 20–22 °C). If this permeability is not reached, several chemical cleaning are then needed to regenerate the membrane and to reach the desired reference permeability of the membrane.

3.5. Critical flux determination: the method of SWB

The square wave barovelocimetry (SWB) technique has been developed by Espinasse et al. [26] and detailed also by the
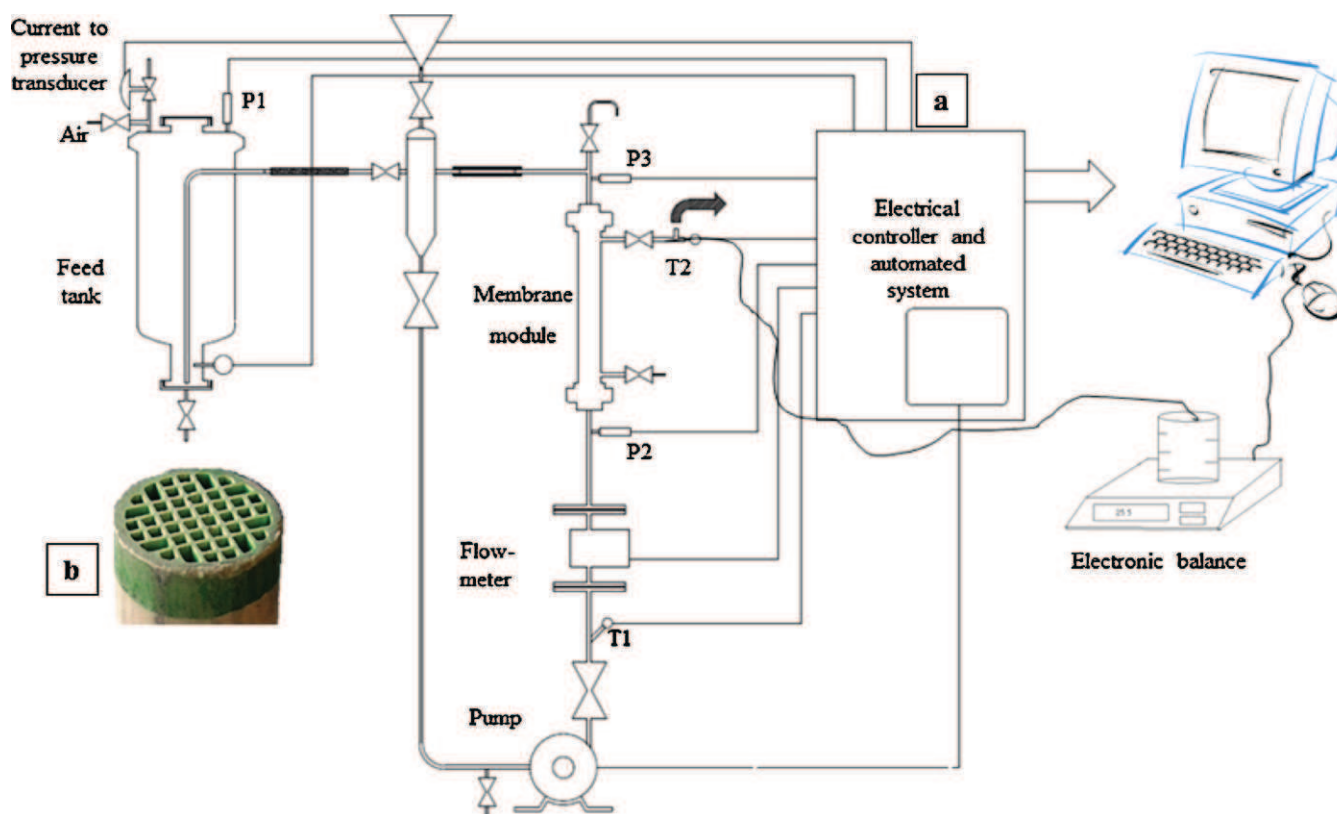
Fig. 3. (a) Scheme of the experimental setup for the critical flux determination and (b) the multi-channel ceramic membrane configuration.
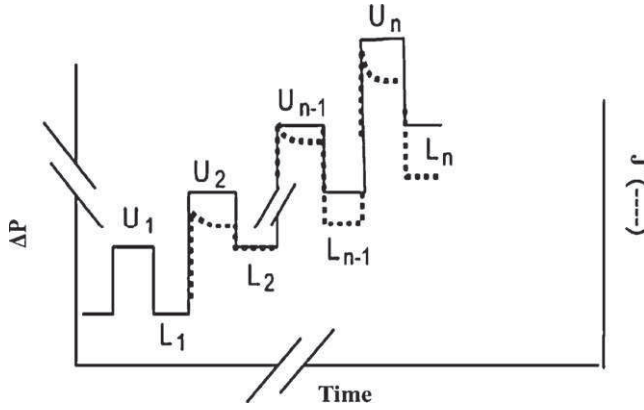
Fig. 4. Square wave barovelocimetry method to measure the critical flux [24].

Fig. 5. Permeate flux and ΔP evolution during filtration of FW and their associated steps numbers.

same authors [27]. The principle of this method is composed of alternative increasing and decreasing pressure steps as shown schematically in Fig. 4. The pressure steps are the alternation of positive and negative variations. The U steps correspond to the upper steps while the L steps correspond to the lower steps. The permeate flux is calculated continuously.

This technique allows the evaluation of the flux loss between two steps of pressure. The flux is compared between steps having the same pressure, for example U_1/L_2 or U_{n-1}/L_n. If the permeate flux is the same at the indicated steps (U_1/L_2), the fouling associated to the step U_2 is considered as totally reversible. If the flux decreases for 2 steps having the same pressure (U_{n-1}/L_n), the fouling associated to the step U_n is considered as partly irreversible. This technique of data treatment allows having accurate values of the critical flux and the rate of irreversibility of the created deposit on the membrane. The number of steps and the corresponding pressures used in this study are summarized in Table 3 corresponding to operating conditions used in wine filtration. Each step lasted for 4 min.

3.6. Calculation method of the irreversible and reversible resistance

The representation of fouling resistance (R_f) versus flux allows the determination of a degree of reversibility of the fouling. The reversible resistance term is used to describe or quantify the portion of the fouling resistance that is eliminated with a decrease in pressure. If R_f at step L_n is equal to R_f at step U_{n-1}, it means that fouling is totally reversible at pressure step n.

The irreversible resistance that appears for an upper pressure step can be reached by comparing the fouling resistance at steps L_n and U_{n-1} steps (Fig. 4). It can be calculated as follow:

$$\frac{r_{if,n}}{R_m} = \left(\frac{R_f}{R_m}\right)_{L_n} - \left(\frac{R_f}{R_m}\right)_{U_{n-1}} \tag{3}$$

where $r_{if,n}$ is the irreversible fouling relative to step n.

In order to calculate the value of the total irreversible fouling (R_{if}) at a given pressure step, all the measured r_{if} at previous steps are summed as follow:

$$R_{if} = (r_{if,n} + r_{if,n-1} + r_{if,n-2} + \ldots) \tag{4}$$

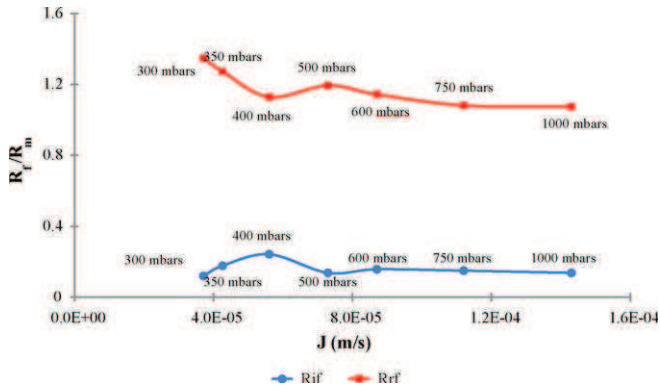The reversible resistance (R_{rf}) can be calculated at each step as follows:

$$\frac{R_{rf}}{R_m} = \frac{R_f}{R_m} - \frac{R_{if}}{R_m} \tag{5}$$

Sometimes, the calculation of the reversible resistance gives negative values which do not have a physical meaning. That could be explained by: (i) the fact that the quasi-steady state of permeate flux is not reached or (ii) the presence of an abnormal increase in fouling resistance (deposit compaction or gelation of the deposit) during the pressure steps. In this case, the reversible resistance is taken at zero and the value of the irreversible resistance is then considered equal to the total fouling resistance.

4. Results

4.1. Determination of the critical flux for filtered wine (FW)

Before investigating the effect of tannins and polysaccharides on critical flux, it is necessary to observe the pattern of permeate flux evolution during the filtration of the "basic matrix" (i.e. the filtered wine FW). Fig. 5 shows the evolution of permeate flux and transmembrane pressure in time while filtering FW. When comparing the value of fluxes for two steps having the same ΔP, fluxes remained almost stables and identical. This point is observed throughout the whole cycle of ΔP stepping. This means that no significant fouling took place. The reversible and irreversible hydraulic resistances deduced from the SWB experiment are plotted in Fig. 6. When the irreversible resistance is equal to zero, it means that the fouling could be considered as totally reversible. In the case of FW, the irreversible resistance is not equal to zero from the beginning of filtration but it remains almost stable and the same throughout the variations of ΔP. This observation could be explained by an adsorption of some wine components on the membrane surface and in the pores. It leads to an increase in the irreversible resistance and decrease in the reversible resistance. The same concept was illustrated in Fig. 1 and it corresponds to the weak form of critical flux. In the case of FW, the critical flux for irreversibility is over the range of the studied conditions ($J_{ci} \geq 1.4 \times 10^{-4}$ m/s).

Table 3
Number of steps and the associated pressure.

Step	1	2	3	4	5	6	7	8	9
Pressure (mbar)	200	250	200	300	250	350	300	400	350
Step	10	11	12	13	14	15	16	17	18
Pressure (mbar)	500	400	600	450	750	600	1000	750	200

Fig. 6. Evolution of reversible R_{rf} and irreversible R_{if} fouling resistance during filtration of FW and the associated transmembrane pressure (mbar).

4.2. Effect of the added molecules

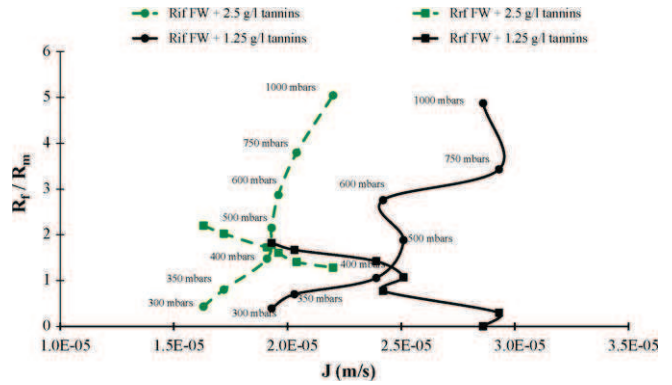### 4.2.1. Impact of tannins on the evolution of the critical flux

Tannins impact on critical flux was studied by adding to FW two different concentrations of tannins: 1.25 g/l and 2.5 g/l. Results of the effect of ΔP stepping on permeate flux are reported in Fig. 7. A net incidence of tannins on permeate fluxes is observed from the beginning of the experiment. The fouling occurs within the first minute of filtration for the two tested concentrations of tannins. The fluxes decrease for the steps having the same ΔP (in example steps 2 and 5). This means that the fouling is partially irreversible. The obtained permeate fluxes are higher for the concentration of 1.25 g/l of tannins (average 2.5×10^{-5} m/s at 1000 mbar (step 16)) than 2.5 g/l (average 1.9×10^{-5} m/s at 1000 mbar). The fluxes are 5–6 times lower than those obtained with FW (1.4×10^{-4} m/s) at 1000 mbar.

Fig. 8 shows the evolution of reversible and irreversible resistance of wines with added tannins. As can be seen, reversible resistance for both tested concentrations decreased while increasing pressure. From the beginning of the experiments, the ratio of irreversible resistance over membrane resistance is not equal to zero. It is equal to 0.39 for FW + 1.25 g/l of tannins and 0.43 for FW + 2.5 g/l of tannins which are twice the irreversible resistance of FW. This means that irreversible fouling occurs within the first minute of filtration. On the other hand, irreversible resistance increased with pressure until reach, at 1000 mbar, 5 times the hydraulic resistance of the membrane for both concentrations.

So, it is obvious that critical fouling conditions are reached from the beginning of the experiments. Therefore, it is only possible to
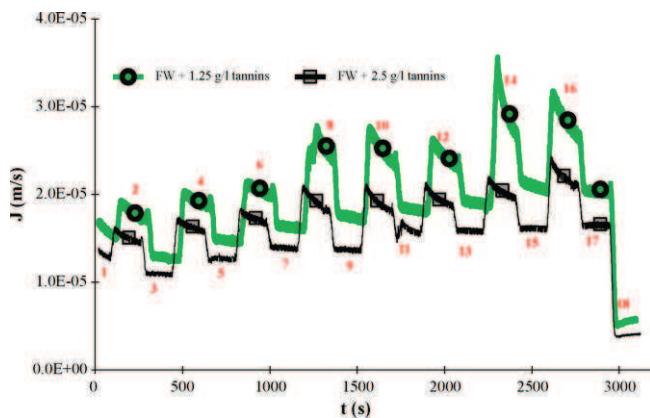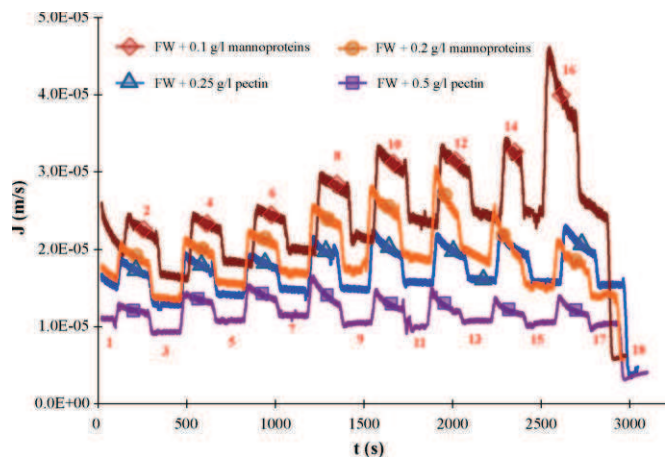

Fig. 8. Impact of tannins on reversible R_{rf} (■) and irreversible R_{if} (●) fouling.

determine the upper limit of the range, where critical flux could be found, in these conditions. This upper limit (not to exceed) is equal to 1.95×10^{-5} m/s for wines containing 1.25 g/l tannins and 1.63×10^{-5} m/s for those containing 2.5 g/l tannins.

4.2.2. Impact of polysaccharides on the evolution of the critical flux

The impact of polysaccharides on critical flux was studied by testing two categories of polysaccharides. The first category includes pectin which comes from grape berries. Pectin effect was studied at 2 concentrations: 0.25 g/l and 0.5 g/l. The second category is formed by mannoproteins whose presence in wine is due to the release from yeast cell wall. The impact of mannoproteins was also studied at two concentrations: 0.1 g/l and 0.2 g/l. Fig. 9 shows the permeate flux evolution of the four filtrations of wine added with polysaccharides. For the tested compounds, results show that fouling occurs from the beginning of the filtration. Also, fluxes are not equal for two steps having the same pressure even at first steps of pressure. This fact means that the determination of a critical flux for each compound at a defined concentration is not feasible for the studied range of pressure. The amount of fouling is different depending on the type of polysaccharides and on its concentration.

The flux evolutions of FW + 0.2 g/l mannoprotein and FW + 0.5 g/l pectin are important to be considered as they provide very special shape of flux versus time and resistance versus flux curves: the initial flux in stepping 1 obtained when processing FW + 0.5 g/l pectin ($J = 1.18 \times 10^{-5}$ m/s) is divided by 2 comparing to that obtained

Fig. 7. Permeate flux evolution during ΔP stepping performed with FW containing 1.25 g/l and 2.5 g/l tannins.

Fig. 9. Permeate flux evolution during ΔP stepping performed with FW + 0.1 g/l mannoproteins, FW + 0.2 g/l mannoproteins, FW + 0.25 g/l pectin and FW + 0.5 g/l pectin.
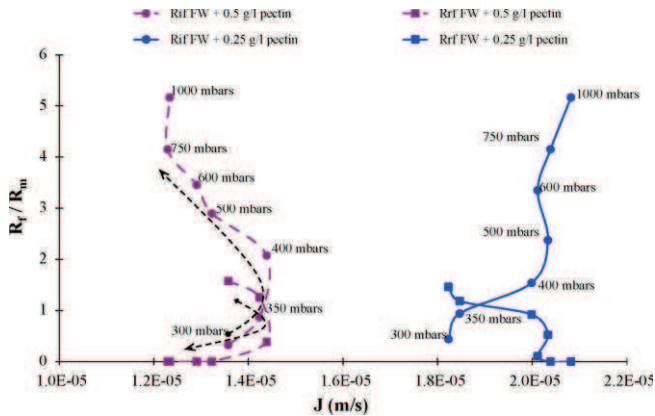
Fig. 10. Pectin's impact on reversible R_{rf} (■) and irreversible R_{if} (●) fouling.

with FW ($J = 2.49 \times 10^{-5}$ m/s). In addition, a little gain in terms of average flux is observed by increasing the transmembrane pressure to reach a maximum of average flux at 400 mbar (step 8 and $J = 1.44 \times 10^{-5}$ m/s). By increasing the pressure beyond 400 mbar, a loss in terms of average flux is observed compared to that obtained at the indicated pressure.

As for FW + 0.5 g/l pectin, the same behaviour has been noticed to FW + 0.2 g/l mannoproteins. The initial permeate flux of FW + 0.2 g/l mannoproteins is higher compared to that obtained with FW + 0.5 g/l pectin. The maximum of average flux ($J = 2.65 \times 10^{-5}$ m/s) is reached at 600 mbar (step 12) for FW + 0.2 g/l mannoprotein. Beyond 600 mbar, permeate flux decreased when increasing the transmembrane pressure.

The evolution of reversible and irreversible resistance during filtration wine added with pectin is illustrated in Fig. 10. The reversible resistance for the FW + 0.25 g/l pectin decreases while increasing pressure and thus the permeate flux until it becomes zero at 600 mbar. The irreversible resistance increases during the experiment to become 5.5 times the membrane resistance at higher pressure. The curves shapes of reversible and irreversible resistance of FW + 0.5 g/l pectin are not common. At the beginning of the filtration, a raise in pressure increases the permeate flux and the irreversible resistance. Beyond 400 mbar ($J = 1.44 \times 10^{-5}$ m/s), a loss in average permeate flux is observed while irreversible resistance continue to increase. It reaches 5.5 times the membrane resistance at higher pressure (1000 mbar). The reversible resistance decreases when increasing the transmembrane pressure and becomes zero at 500 mbar. Therefore, beyond this pressure, the irreversible resistance becomes equal to the total resistance.
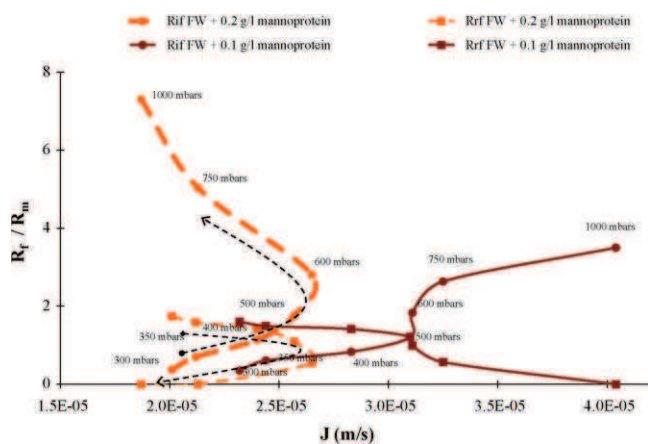

Fig. 11. Mannoproteins' impact on reversible R_{rf} (■) and irreversible R_{if} (●) fouling.

Fig. 11 shows the impact of added mannoprotein on the evolution of reversible and irreversible resistance. For FW + 0.1 g/l mannoprotein, the evolution of both resistances is similar to that obtained with tannins and 0.25 g/l pectin. Irreversible resistance reaches about 4 times the membrane resistance. In the case of FW + 0.2 g/l mannoprotein, the curves shapes of both resistance look like those obtained with 0.5 g/l pectin. The difference is the inflexion point which is obtained at 600 mbar ($J = 2.55 \times 10^{-5}$ m/s). Irreversible resistance reaches in this case 7.5 times membrane resistance.

5. Discussion

In the present study, experiments were realized in order to determine the critical flux for irreversibility J_{ci} in wine cross-flow microfiltration. For colloidal filtration, this term is the more appropriate because it discriminates between reversible and irreversible fouling. When filtering colloidal dispersion, fouling cannot be totally avoided due to the phenomenon of the concentration polarization and in some cases adsorption on membrane material. But, the coagulation of dispersed phase close to the membrane surface, followed by deposition upon it, can be avoided.

In wine, tannins, pectin and mannoprotein present colloidal behaviours. In theory, when filtering below the critical flux for irreversibility, irreversible fouling by wine colloids can be prevented. In our experiments, no critical flux for irreversibility could be determined for the wine colloids for the studied range of pressures which are the same used in wine filtration. All tested molecules, whatever the concentration, exhibit irreversible fouling even at very low pressures.

For wine tannins, it was demonstrated that their adsorption on membrane surface occurs in static conditions [9,10]. Under dynamic conditions, tannins tend to accumulate at the pore entrance on the membrane feed side [9]. It seems also, according to Fig. 8, that the rate of fouling and its type is strongly influenced by the transmembrane pressure. The increase in irreversible fouling can be explained by the transition between the state of dispersed molecules to aggregates. This fact is promoted by the increase of the transmembrane pressure which forces the molecules to be near the membrane surface and promotes membrane/tannins and tannins/tannins interactions.

Wine polysaccharides have been identified to play a major role in membrane fouling during cross-flow microfiltration of wine [4–10]. According to the results presented in Section 4.2.2, fouling by polysaccharides cannot be avoided. It was shown that under static conditions polysaccharides adsorption is negligible [7]. In dynamic conditions, polysaccharides adsorption tends to be governed by the hydrophobic/hydrophilic character of the membrane [10] as well as by membrane polarity [7]. In most fruit juices, pectin (a well-known gelling agent) forms a gel-layer on the membrane surface [28–31]. The formation of this layer is enhanced by the process. Kirk et al. [32] as well as Szaniawski and Spencer [33] showed a bell shaped profile when plotting permeate flux versus TMP during the filtration of solutions rich in pectin. These observations were explained as following: an increase in pressure would cause the macromolecules which are already on the membrane surface to pack more tightly; At high pressures, the densely packed pectin molecules form a barrier across the membrane and prevent the flow of permeate flux. This barrier was identified as gel-layer [34]. During filtration of solutions containing pectin, Rai et al. [35] showed that an increase in pressure lead to an increase in flux till a limit where a gel-type layer grows rapidly because if the enhanced forced convection of the solutes towards membrane. Pectin hydrolysis by pectinases leads to an improvement of the permeate flux [36].
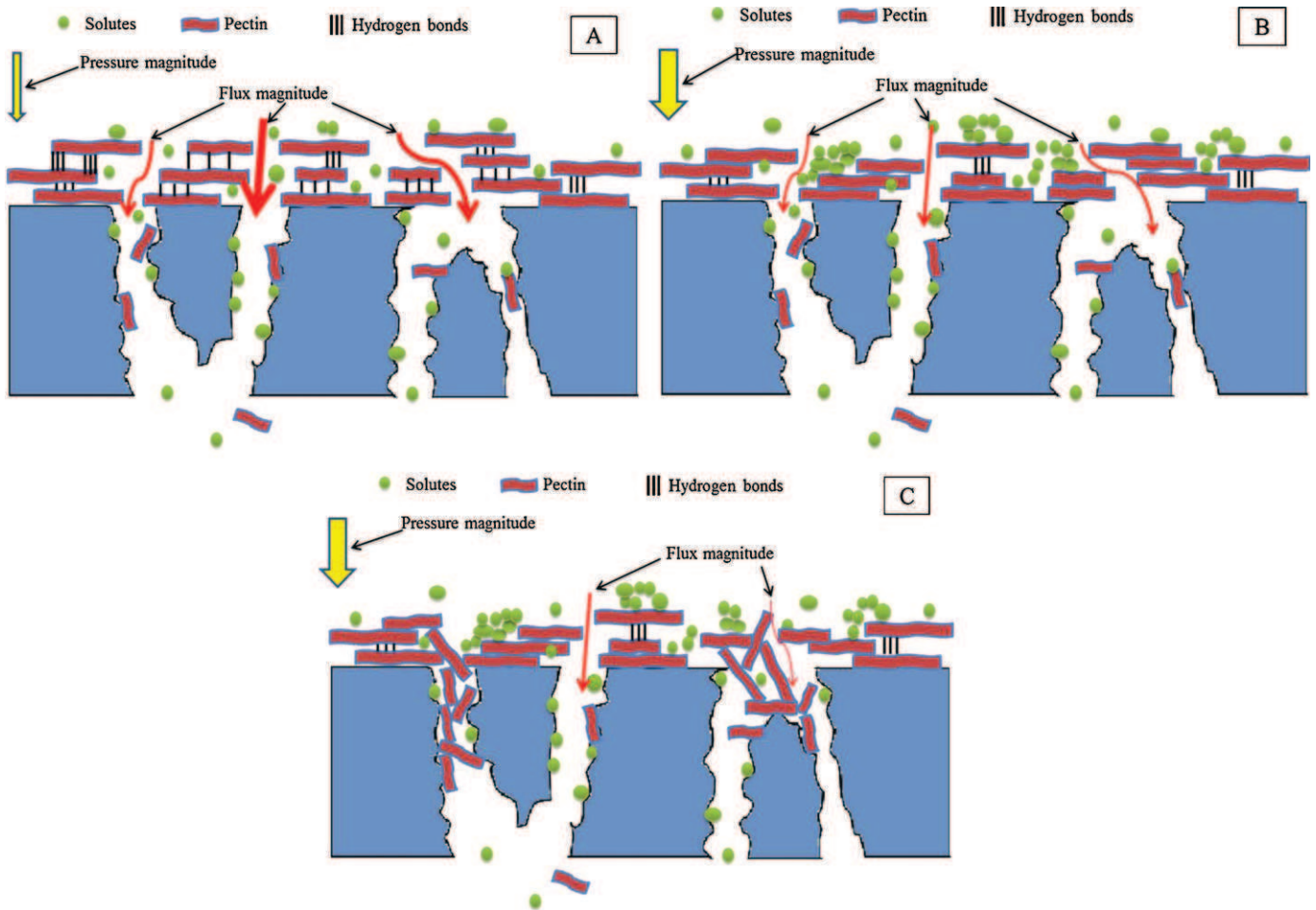
Fig. 12. (A) Pectic gel layer at membrane surface, (B) pectic gel layer compaction, and (C) unstructured pectic gel layer.

An unexpected phenomenon occurred when filtering FW + 0.5 g/l pectin and FW + 0.2 g/l mannoproteins (cf. Fig. 9). After a given level of pressure, the average permeate flux begin to decrease with increasing pressure. In fact, Kirk et al. [32] showed that pectin forms an elastic pectic gel layer which is evidenced by the partial restoration of permeate flux upon gradual release of the transmembrane pressure. This highlights that the pectic gel could be compressible. In our study, the following explanation can be proposed. The gel layer was compressible till a limit of pressure. Beyond this limit, hydrogen bond bridges, that transform the pectic chains into gel aggregates (Fig. 12A), collapse leading to the closure of interstitial spaces between the chains (Fig. 12B). The gel layer can also be unstructured under pressure and fill partially the pores leading to an additional fouling increase (Fig. 12C). So, the compacted pectic gel layer acts as a second membrane and may retain other solutes. This explains the results obtained with FW + 0.5 g/l pectin.

Mannoproteins impact on membrane fouling was little studied in the literature. It was shown that mannoproteins might cause the strongest decrease in wine filterability [8]. Mannoproteins are not a gelling agent and do not form a gel-like structure over the membrane. Mannoproteins seem to form a deposit at the membrane surface. The results obtained when filtering FW + 0.2 g/l mannoproteins could be also explained by a compressible cake where the spaces between molecules are reduced with the pressure increase.

These results highlight that the critical flux concept is inappropriate to be industrially applied to wine cross-flow microfiltration within the classical range of operation. Therefore, other concepts should be taken into consideration like "threshold flux" term. It is defined as the flux at or below which membrane system will generate a low rate of fouling and fluxes remain acceptable but above which the rate of fouling increases markedly [22]. This definition was used firstly for "sustainable flux" but the concept of the latter is modified and includes economic factors. So, this concept is useful to define regions of low and high fouling. The criteria and aspects to define this threshold flux may vary depending on what the researchers are seeking. The criterion defined in this study is based on the ratio between irreversible resistance and the hydraulic membrane resistance and it is defined as: "the flux at which the ratio R_{if}/R_m is inferior to 1".

Fig. 13 showed the criterion ($R_{if}/R_m \leq 1$) used to determine the threshold flux and comparison of the obtained flux with the critical flux of irreversibility (J_{ci}). The data shown in Fig. 13 except for FW represent the higher limit of the range that could be obtained under the defined conditions.

The threshold fluxes for all the filtrations are higher than those obtained with the critical flux concept, even with a certain degree of fouling. The gain in fluxes may reach 34% in the case of FW+ 0.1 g/l mannoprotein. In the cases of FW + 0.5 g/l pectin and FW + 0.2 g/l mannoprotein, critical flux for irreversibility could not be determined but a threshold flux could be obtained. In other hand, the critical and threshold fluxes are still much lower than those obtained with FW which are higher than 1.4×10^{-4} m/s.
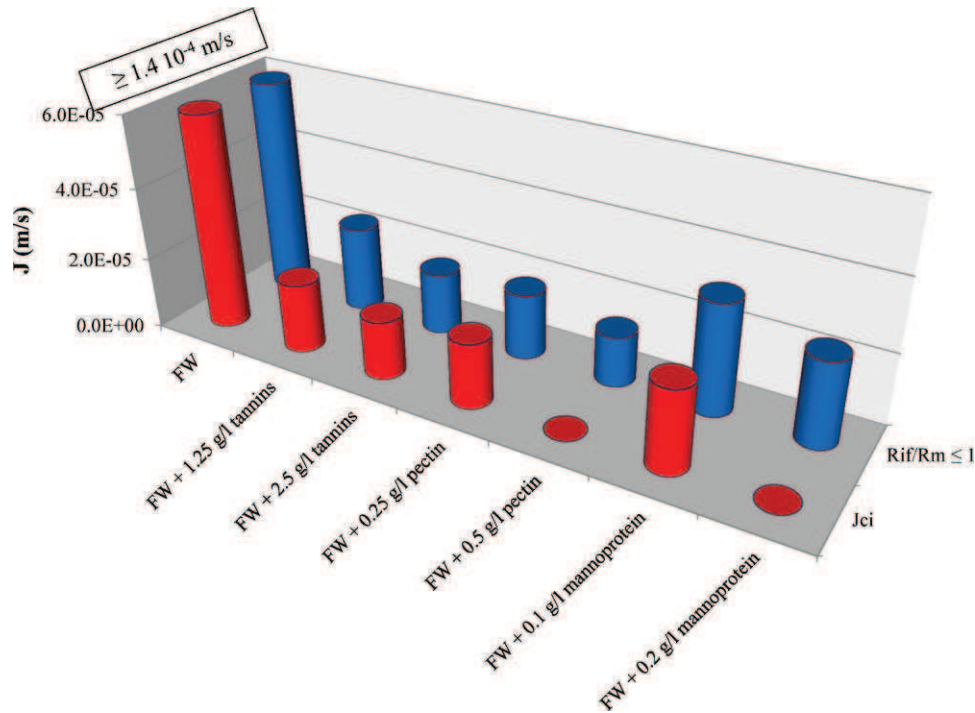
Fig. 13. Comparison of critical flux for irreversibility (the bar gives here the lower value of critical flux for FW and the upper value of critical flux for FW with added molecules) and the threshold flux.

6. Conclusion

In this study, critical operating conditions during wine cross-flow microfiltration were studied. The square wave barovelocimetry (SWB) was used to assess the evolution of reversible and irreversible resistance with permeate flux. It allows the determination of critical flux for irreversibility (J_{ci}). For all tested macromolecules (tannins, pectin and mannoproteins) and associate concentrations, no clear critical flux for irreversibility can be really determined in the range of tested pressures: this study determines then the upper value of the critical flux. In fact, membrane fouling in presence of these wine molecules occurs from the first minute of filtration. This work shows the importance of tannins, pectin and mannoprotein on the membrane fouling for concentration ranges classically found in wine. The main fouling mechanisms are adsorption on membrane material as showed with FW solution and formation of deposit layer as proposed for FW + 0.2 g/l mannoproteins. A gel layer compaction or deformation under high pressures is proposed to explain the phenomenon observed with FW + 0.5 g/l pectin. New criteria were used in order to determine a "threshold flux" where a certain degree of fouling is acceptable. It leads to a convenient set of operating conditions compatible with industrial constraints.

Nomenclature

ΔP	transmembrane pressure (Pa)
$\Delta \Pi$	osmotic pressure (Pa)
μ	permeate viscosity (Pa s)
FW	filtered wine
J	permeate flux (m/s)
J_{ci}	critical flux for irreversibility (m/s)
IC	colour intensity
R_m	membrane hydraulic resistance (m^{-1})
R_{ads}	resistance due to adsorption (m^{-1})
R_{rf}	reversible resistance (m^{-1})
R_{if}	irreversible resistance (m^{-1})
SWB	square wave barovelocimetry
TPI	total polyphenol index

References

[1] A.G. Cook, P. Weinstein, J.A. Centeno, Health effects of natural dusts: role of trace elements and compounds, Biol. Trace Elem. Res. 103 (2005) 1–15.

[2] A. Lüdemann, Wine clarification with a cross-flow microfiltration system, Am. J. Enol. Viticult. 38 (1987) 228–235.

[3] G. Belfort, R.H. Davis, A.L. Zydney, The behaviour of suspensions and macromolecules solutions in cross-flow microfiltration, J. Membr. Sci. 96 (1994) 1–58.

[4] Q. Gan, R.W. Field, M.R. Bird, R. England, J.A. Howell, M.T. McKechnie, C.L. Oshaughnessy, Beer clarification by cross-flow microfiltration: fouling mechanisms and flux enhancement, Chem. Eng. Res. Des. 75 (1997) 3–8.

[5] M.P. Belleville, J.M. Brillouet, B.T. Delafuente, M. Moutounet, Fouling colloids during microporous alumina membrane filtration of wine, J. Food Sci. 57 (1992) 396–400.

[6] P.J. Cameira Dos Santos, Colmatage en microfiltration tangentielle: mise en evidence d'interactions entre les polysaccharides et les polyphénols d'un vin et des membranes polymériques, Ph. D. Thesis. University of Montpellier II. Ecole Nationale Supérieure Agronomique de Montpellier, 1995.

[7] M.N. Vernhet, J.M. BellonFontaine, E. Brillouet, M. Roesink, Moutounet, Wetting properties of microfiltration membrane: determination by means of the capillary rise technique and incidence on the adsorption of wine polysaccharide and tannins, J. Membr. Sci. 128 (1997) 163–174.

[8] A. Vernhet, P. Pellerin, M.P. Belleville, J. Planque, M. Moutounet, Relative impact of major wine polysaccharides on the performances of an organic microfiltration membrane, Am. J. Enol. Viticult. 50 (1999) 51–56.

[9] M. Vernhet, Moutounet, Fouling of organic microfiltration membranes by wine constituents: importance, relative impact of wine polysccharides and polyphenols and incidence of membrane properties, J. Membr. Sci. 201 (2002) 103–122.

[10] M. Ulbricht, W. Ansorge, I. Danielzik, M. Konig, O. Schuster, Fouling in micro-filtration of wine: the influence of the membrane polymer on adsorption of polyphenols and polysaccharides, Separ. Purif. Technol. 68 (2009) 335–342.

[11] P. Bacchin, P. Aimar, R.W. Field, Critical and sustainable fluxes: theory, experiments and applications, J. Membr. Sci. 281 (2006) 42–69.

[12] G. Gésan-Guiziou, E. Boyaval, G. Daufin, Critical stability conditions in cross-flux microfiltration of skimmed milk: transition to irreversible deposition, J. Membr. Sci. 158 (1999) 211–222.

[13] W. Youravong, M.J. Lewis, A.S. Grandison, Critical flux in ultrafiltration of skimmed milk, Food Bioprod. Process. 81 (2003) 303–308.

[14] J. De Bruijin, R. Borquez, Analysis of the fouling mechanisms during cross-flow ultrafiltration of apple juice, LWT 39 (2006) 861–871.

[15] P. Bacchin, P. Aimar, V. Sanchez, Model for colloidal fouling of membranes, AICHE J. 41 (1995) 368–377.

[16] R.W. Field, D. Wu, J.A. Howell, B.B. Gupta, Critical flux concept for microfiltration fouling, J. Membr. Sci. 100 (1995) 259–272.

[17] J.A. Howell, Sub-critical flux operation in microfiltration, J. Membr. Sci. 107 (1995) 165–171.

[18] D.X. Wu, J.A. Howell, R.W. Field, Critical flux measurement for model colloids, J. Membr. Sci. 152 (1999) 89–98.

[19] L. Defrance, M.Y. Jaffrin, Comparison between filtrations at fixed trans-membrane pressure and fixed permeate flux: application to a membrane bioreactor used for wastewater treatment, J. Membr. Sci. 152 (1999) 203–210.

[20] A.G. Fane, Sustainability and membrane processing of wastewater for reuse, Desalination 202 (2007) 53–58.

[21] P. Le-Clech, V. Chen, T. Fane, Fouling in membrane bioreactors used in wastewater treatment, J. Membr. Sci. 284 (2006) 17–53.

[22] R.W. Field, G.K. Pearce, Critical, sustainable and threshold fluxes for membrane filtration with water industry applications, Adv. Colloid Interface Sci. 164 (2011) 38–44.

[23] L. Usseglio-Tomasset, Les colloïdes glucidiques solubles des moûts et des vins, Connaissance de la vigne et du vin 10 (1976) 193–226.

[24] P. Ribéreau-Gayon, Y. Glories, A. Maujean, D. dubourdieu, Handbook of enology volume 2: the chemistry of wine, stabilization and treatments, 2nd edition, Dunod, Paris, 2006.

[25] C. Flanzy, Œnologie: fondements scientifiques et technologiques, Lavoisier TEC & DOC, Paris, 1998.

[26] B. Espinasse, P. Bacchin, P. Aimar, On an experimental method to measure critical flux in ultrafiltration, Desalintaion 146 (2002) 91–96.

[27] B. Espinasse, P. Bacchin, P. Aimar, Filtration method characterizing the reversibility of colloidal fouling layers at a membrane surface: analysis through critical flux and osmotic pressure, J. Colloid Interface Sci. 320 (2008) 483–490.

[28] M.Z. Sulaiman, N.M. Sulaiman, L.Y. Shih, Limiting permeate flux in the clarification of untreated starfruit juice by membrane ultrafiltration, J. Chem. Eng. 68 (1998) 145–148.

[29] M.Z. Sulaiman, N.M. Sulaiman, M. Shamel, Ultrafiltration studies on solutions of pectin, glucose and their mixtures in a pilot scale crossflow membrane unit, J. Chem. Eng. 84 (2001) 557–563.

[30] P. Rai, G.C. Majumdar, S. Dasgupta, S. De, Modeling of sucrose permeation though a pectin gel during ultrafiltration of depectinized mosambi [Citrus sinensis (L.) Osbeck] juice, J. Food Sci. 71 (2006) 87–94.

[31] P. Rai, G.C. Majumdar, S. Dasgupta, S. De, Modeling of permeate flux of synthetic fruit juice and mosambi juice (Citrus sinensis (L.) Osbeck) in stirred continuous ultrafiltration, LWT 40 (2007) 1765–1773.

[32] D.E. Kirk, M.W. Montgomery, M.G. Kortekaas, Clarification of pear juice by hollow fiber ultrafiltration, J. Food Sci. 48 (1983) 1663–1667.

[33] A.R. Szaniawski, H.G. Spencer, Microfiltrtaion of pectin solutions by a titanium dioxide membrane, Key Eng. Mater. 61/62 (1991) 243–248.

[34] R. Jiraratananon, A. Chanachai, A study of fouling in the ultrafiltration of passion fruit juice, J. Membr. Sci. 111 (1996) 39–48.

[35] P. Rai, G.C. Majumdar, S. Dasgupta, S. De, Understanding ultrafiltration performance with mosambi juice in an unstirred batch cell, J. Food Process. Eng. 28 (2005) 166–180.

[36] F. Vaillant, P. Millan, G. O'Brien, M. Dornier, M. Decloux, M. Reynes, Cross flow microfiltration of passion fruit juice after partial enzymatic liquefaction, J. Food Eng. 42 (1999) 215–224.